ONLINE ICRC 2021
THE ASTROPARTICLE PHYSICS CONFERENCE
Berlin | Germany
37th International
Cosmic Ray Conference
12–23 July 2021

Determination of Expected TIGERISS Observations

Brian F. Rauch[a], Nathan E. Walsh[a] and Wolfgang V. Zober[a] for the TIGERISS Collaboration
[a]Department of Physics and McDonnell Center for the Space Sciences, Washington University, St. Louis, MO 63130 USA

Work shown here supported by the McDonnell Center for the Space Sciences and the Peggy and Steve Fossett Foundation

Abstract

We present the method used to estimate the cosmic-ray observations expected for that the Trans-Iron Galactic Element Recorder for the International Space Station (TIGERISS), which is designed to measure the abundances of the rare Ultra-Heavy Galactic Cosmic Rays (UHCR) $_{30}$Zn and heavier. TIGERISS uses planes of crossed silicon strip detectors at the top and bottom for charge and trajectory determination and acrylic and aerogel Cherenkov detectors for velocity and charge determination. Instruments are modeled in configurations for the Japanese Experiment Module (JEM) "Kibo" Exposed Facility (∼1.66 m^2 sr), as an European Space Agency Columbus Laboratory external payload (∼1.16 m^2 sr), and as an ExPRESS Logistics Carrier (ELC) experiment (∼1.10 m^2 sr). Differential geometry factors determined for detector orientations within the geomagnetic field over the ISS 51.6° inclination orbit are used to determine geomagnetic screening. Energy spectra are integrated using the higher of the energies needed to trigger the instrument or penetrate the geomagnetic field for time-weighted bins of geomagnetic latitude, instrument orientation, and incidence angle. Finally, abundances are reduced by the fraction of events calculated to fragment in the instrument.

TIGERISS Instrument

TIGERISS is an evolutionary development of the TIGER family of instruments with improved charge resolution and dynamic range. TIGERISS utilizes three basic detector subsystems to unambiguously measure the charge of all GCRs from $_5$B to $_{82}$Pb with energy greater than ∼ 0.2 GeV/nucleon. Silicon strip detector (SSD) arrays at the top and bottom of the instrument measure particle trajectories and ionization energy deposits (dE/dx). Two Cherenkov (CK) detectors measure nuclear charge (Z) and velocity (β): C1 with an acrylic radiator (optical index of refraction $n = 1.49$) and C0 with a silica aerogel radiator ($n = 1.04$). Figure 1 below shows the TIGERISS instrument model for the JEM-EF configuration (left) and mounted in a JEM-EF pallet (right). The integrated geometry factors are given in Figure 2 for JEM-EF (left), ELC (middle), and Columbus Laboratory (right) TIGERISS configurations, showing that most of the acceptance is within ∼60°.

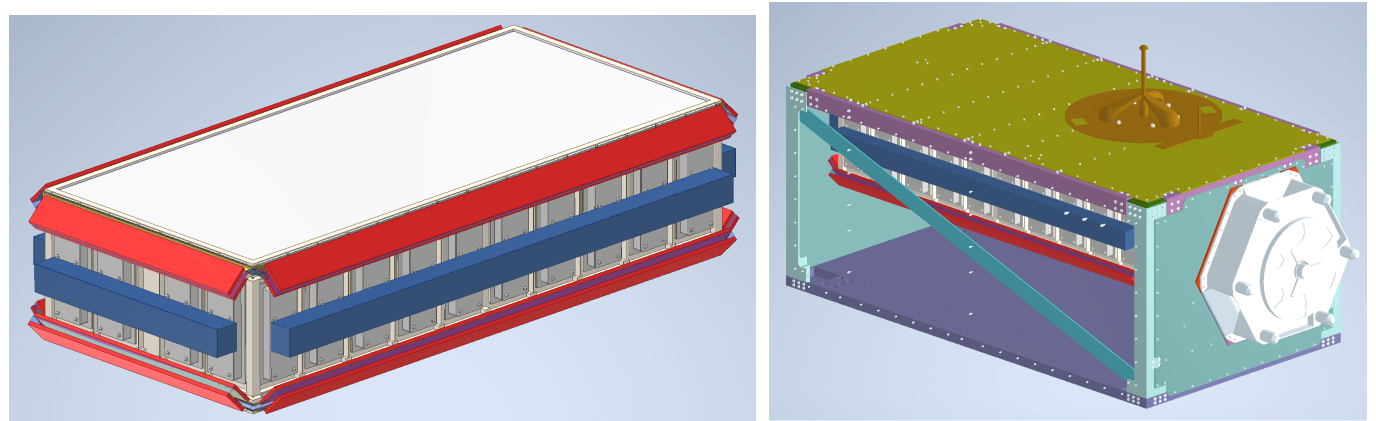

Figure 1: Technical model of TIGERISS detector stack (left). TIGERISS instrument model shown mounted on the JEM-EF pallet (right), with ample space for thermal, power and electronics systems. The results shown assume detector dimensions that are compatible with the ISSCREAM JEM-EF mounting location.

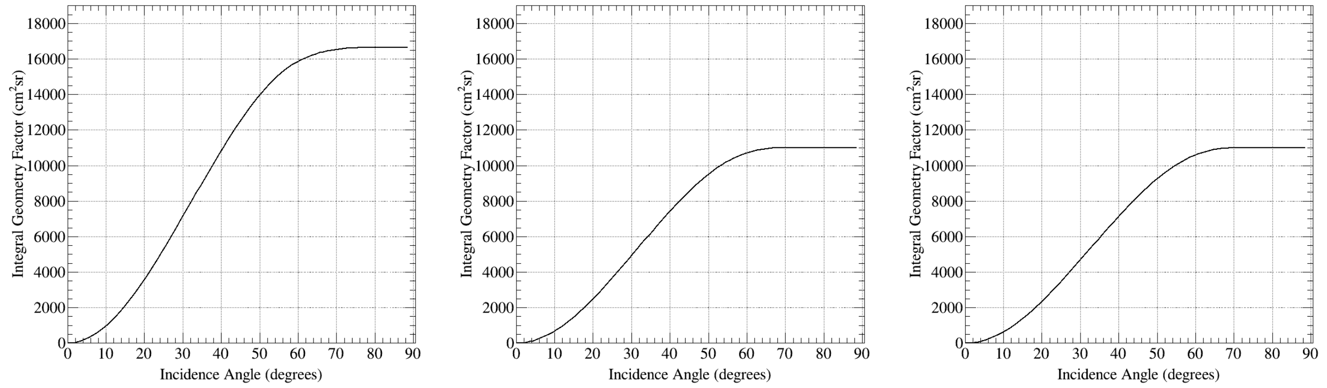

Figure 2: Left to right: JEM-EF configuration 167.0 cm(L) 67.0 cm(W) 40.0 cm(T) ∼1.66 m^2 sr, ExPRESS Logistics Carrier (ELC) 105.0 cm(L) 75.0 cm(W) 40.0 cm(T) ∼1.10 m^2 sr, and ESA Columbus Laboratory external payload 97.79 cm(L) 74.93 cm(W) 35.08 cm(T) ∼1.16 m^2 sr.

Modelling Geomagnetic Screening

Geomagnetic screening is based on the geomagnetic latitudes sampled by the ISS orbit and the screening threshold strength as a function of East-West angle, shown below in the left and right plots of Figure 3, respectively.

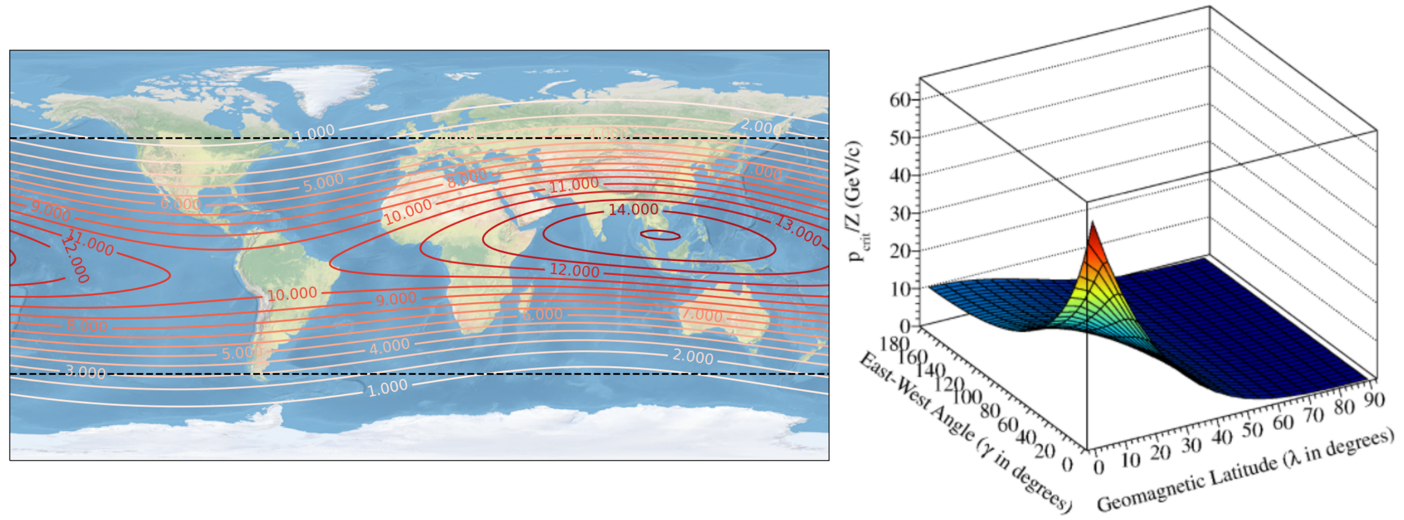

Figure 3: The geomagnetic latitudes correspond to different vertical cutoff rigidities. The critical momentum needed to penetrate the geomagnetic field scales with the geomagnetic latitude and East-West angle as shown in the figure.

ISS Orbit Weighted Vertical Cutoff Rigidities

The orbital residence time at geomagnetic latitudes is used to find the weighted vertical cutoff rigidities shown in Figure 4. Energy thresholds as a function of East-West angle are derived from the trajectory dependent critical momentum (Figure 3). The higher of the rigidity or detector threshold are used to evaluate integral spectra derived from differential spectra shown in Figure 5 weighted by relative abundances [1].

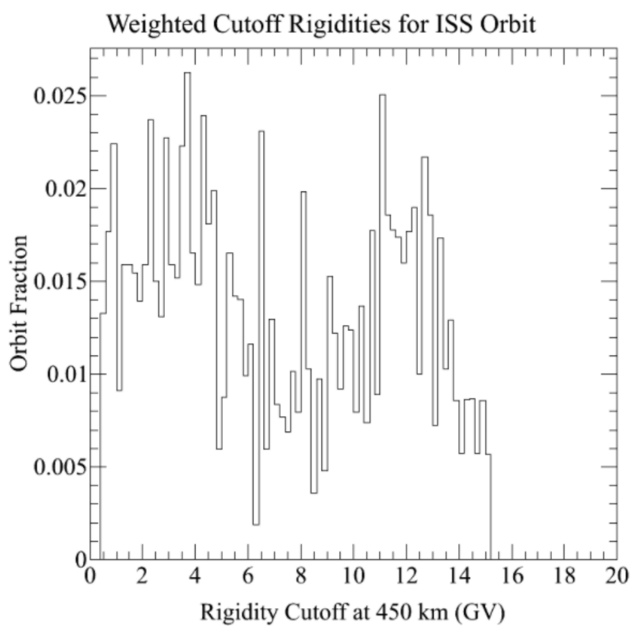

Figure 4: The fraction of the ISS orbit spent at each vertical cutoff rigidity.

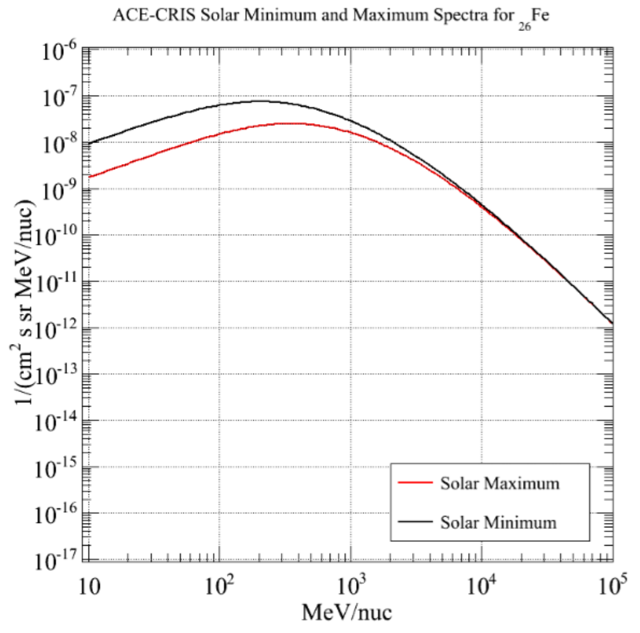

Figure 5: The solar maximum and minimum iron spectra are integrated and scaled using relative abundances of heavier elements.

References

[1] W. R. Binns et al. Abundances of Ultraheavy Elements in the Cosmic Radiation: Results from HEAO 3. *The Astrophysical Journal*, 346:997–1009, 1989.

[2] N. E. Walsh. *SuperTIGER Elemental Abundances for the Charge Range* $41 \leq Z \leq 56$. PhD thesis, Washington University in St. Louis, 2020.

East-West differential geometry factor

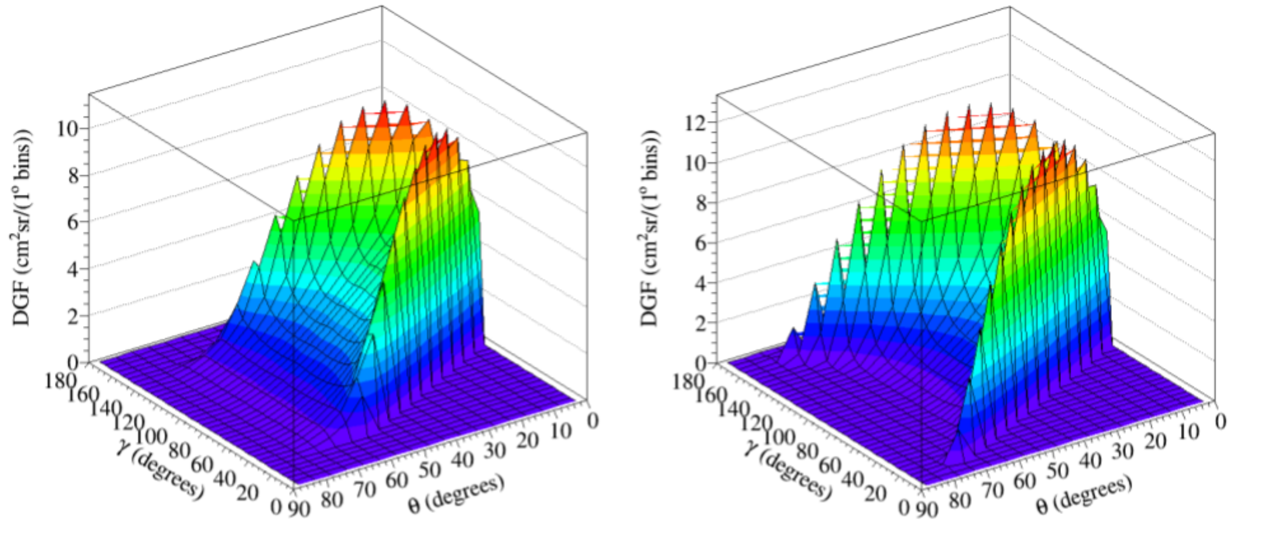

Figure 6: The TIGERISS instrument differential geometry factor is mapped over all possible particle incidence angles (θ) and East-West angles (γ) and modelled for all ISS inclination angles with 1 degree resolution. Two such maps are shown, in which the East-West angle is aligned with the instrument major (left) and minor (right) axes.

Predicted Abundances After 1 Year

For a given element, the predicted observed abundance after 1 year of exposure time is calculated using the scaled integral spectrum of the element (derived from Figure 5), evaluated at the energy corresponding to the critical momentum at each geomagnetic latitude (Figure 3), given the weighted rigidity orbit fraction at the vertical cutoff rigidity (Figure 4) and the differential geometry factor for the incidence angle and East-West angle in question (Figure 6). The elemental abundances predicted for the TIGERISS instrument after 1 year of operation on the ISS at average and maximum solar activity are compared to those measured by SuperTIGER during its 55 day long-duration-balloon flight [2].

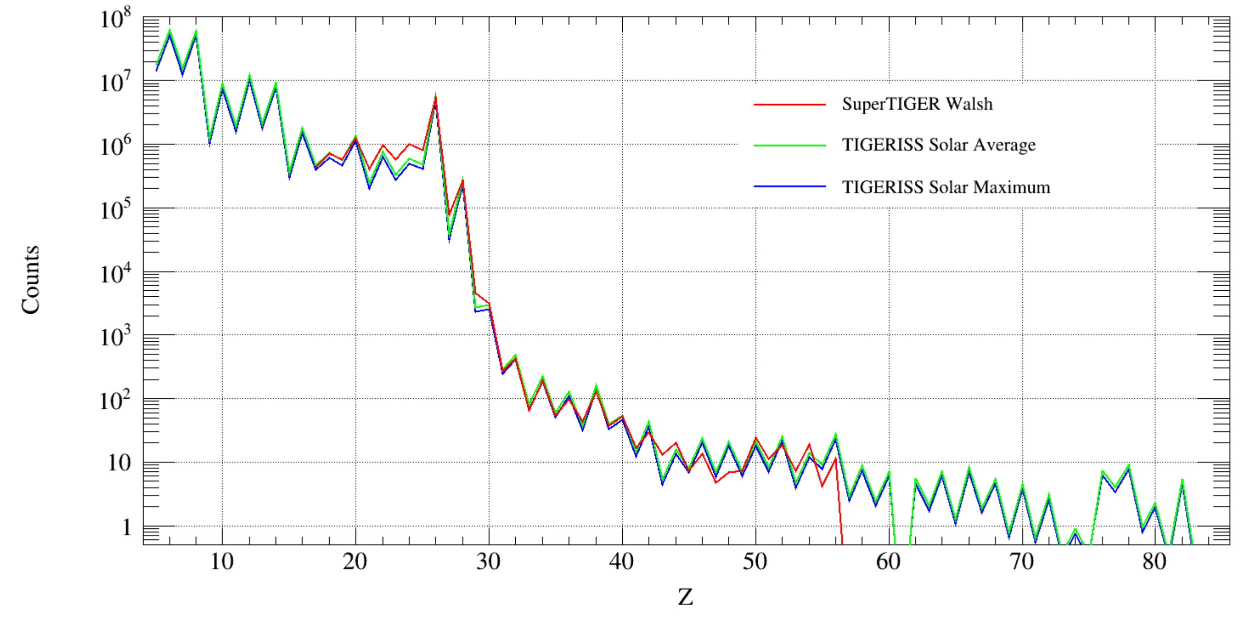

Figure 7: Predicted abundances measured by TIGERISS after 1 year of operation are comparable to those measured by SuperTIGER over its 55 day long-duration-balloon flight [2].